JCARME
ISSN: 2228-7922
Journal of Computational and Applied Research in Mechanical Engineering
Vol. 4, No. 1, pp. 43- 54, Autumn 2014
http://jcarme.srttu.edu

# A numerical and experimental study on buckling and post-buckling of cracked plates under axial compression load

**M. Shariati[a, *], A. M. Majd Sabeti[b] and H. Gharooni[b]**

[a] *Department of Mechanical Engineering, Ferdowsi University of Mashhad, Mashhad, Iran*
[b] *Department of Mechanical Engineering, Shahrood University of Technology, Shahrood, Iran*

**Article info:**
Received: 10/12/2012
Accepted: 08/03/2013
Online: 11/09/2014

**Keywords:**
Cracked plate,
Buckling,
Post-buckling,
Experimental method,
FEM.

**Abstract**
Existence of cracks in industrial structures is one of the important causes of their failure, especially when they are subjected to important axial compressive forces that might lead to buckling. Therefore, it must be considered in stress analysis and designing and loading of such structures. In this paper, the buckling and post-buckling behaviors of stainless-steel cracked plates under axial compression load were investigated both experimentally and numerically and effects of the geometrical and mechanical parameters, such as crack length, crack angle, crack position, plate imperfection, load band, and plate thickness on the critical buckling load were studied. In the experimental study, mechanical properties and plastic behavior of stainless steel plates were determined for the subsequent numerical study. Numerical modeling was carried out by ABAQUS finite element software. Numerical predictions were compared with the experimental results and the reliability of the numerical solution was proven. Results demonstrated the considerable effects of the mentioned parameters on the critical buckling load of plate.

**Nomenclature**

| | | | |
|---|---|---|---|
| a | Crack length | E | Modulus of elasticity |
| W | Half of plate width | $\sigma_y$ | Yield stress |
| L | Half of plate length | $\nu$ | Poisson's ratio |
| t | Plate thickness | $\varphi$ | Load proportion |
| $\theta$ | Crack angle | $W_p$ | Half of axial load width |

## 1. Introduction

Presence of cracks in thin-walled structures, such as plates and shells used in different engineering applications, is a quite common situation. Nowadays, investigating the buckling and post-buckling phenomena in these structures such as cracked plates is essential for their structural safety assessment in the field of mechanics, aerospace, and ship-building.

*Corresponding author
*Email address: mshariati44@gmail.com*

Buckling usually occurs due to the presence of tension, compression, and shear loading. Upon the increase of these forces and their arrival at the critical limit, the plate begins to buckle, which causes in-plane and out-of-plane displacement in the plates. It is worth mentioning that buckling occurs under tension in plates which have cracks or cut-outs.

In recent years, one of the matters attracting the attention of researchers and engineers has been the buckling of cracked plates; but, few articles have been presented in this field. Sih and Lee studied the behavior of cracked plates under tension and compression loads and the effect of crack length on the quantity of critical load and then displayed the mode shapes related to these plates [1]. Shaw and Huang studied the behavior of cracked plates under uniaxial tension force using the finite element method and examined the effect of crack length, boundary condition, and loading on buckling load [2]. Riks et al. studied the buckling and post-buckling of cracked plates under tensile load using the finite element method [3]. Their results indicated that the stress intensity factor in post-buckling always adopts higher quantity than stress intensity factor in pre-buckling. Guz and Dyshel studied the two-layer metal plates (steel-aluminium alloy) with crack under tension and examined the critical stresses in the onset of buckling and the concerned deformations [4]. Satish Kumar and Paik computed the buckling load for plates with central crack and edge crack under uniaxial compressive load, biaxial compressive load, and in-plane shear load by applying hierarchical trigonometric functions [5]. They proved the validity of their relations through finite element method. Brighetni used the numerical finite element method and also analytical method to study the phenomenon of buckling in cracked plates under tensile and compressive loads [6-8]. He investigated the effect of mechanical and geometrical variables such as Poisson's ratio, boundary conditions, crack length, and crack angle on buckling load. His results indicated that each of these parameters has a considerable effect on buckling load. Alinia et al. reviewed the cracked plates under shear load using the finite element method and also the effect of some of the mechanical and geometrical specifications in the behavior of these plates [9 and 10]. They also studied the sensitivity of the inferred results to the type of element-setting. Shariati et al. numerically studied the buckling and post-buckling of cracked plates under axial compression loading in elastic-plastic materials by considering some parameters, such as crack length, crack angle, boundary conditions, imperfection, and different materials of plates [11].

A glance at the presented articles shows that, while the effect of each of the mentioned factors is very important for the critical buckling load, the buckling and post-buckling of cracked plates under the compression load and the effect of such parameters as crack length, crack angle, crack position, load band, plate imperfection, and plate thickness have not been studied and reviewed in this phenomenon.

In this research, the buckling and post-buckling of cracked plates under axial compression load were experimentally and numerically studied. Furthermore, effects of the mentioned parameters on the critical buckling load were investigated. The mechanical properties and plastic behavior of the stainless steel plates for three different thicknesses were also determined for the subsequent numerical solution and buckling experiments were conducted. Numerical modeling was carried out by ABAQUS finite element software. Numerical predictions were compared with the experimental results and the reliability of the numerical solution was proven. Furthermore, effect of the initial imperfection of the specimens, which is regarded as the percentage of the plate thickness, was studied as one of the effective parameters on the critical buckling load of cracked plates.

## 2. Experimental study

### *2.1. Specimen geometry*

Geometry of the studied rectangular plate along with central and edge cracks under compression load is shown in Fig. 1(a). In this figure, "2W" and "2L" stand for the width and length of the plate, respectively. Their quantities are equal to

100 mm and 200 mm, respectively. "t" stands for plate thickness, and "θ" and "2a" are crack angle and crack length, respectively, adopting various quantities. Angle of the unilateral and bilateral edge cracks which are shown in Fig. 1(b and c) is equal to zero.

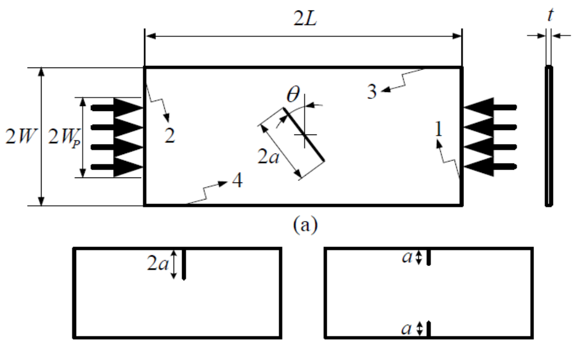


**Fig. 1.** Studied geometry; rectangular plates under axial compression load with: (a) Central crack; (b) Unilateral edge crack; (c) Bilateral edge crack.

*2.2. Mechanical properties of material*

This study analyzed the buckling and post-buckling behaviors of stainless steel 304 cracked plates under axial compression load. Mechanical properties of the steel plates were obtained by the uniaxial tension test according to ASTM E8 standards using INSTRON machine. In Fig. 2, the condition of mounting the standard tension specimens on INSTRON machine is demonstrated. Mechanical properties of stainless steel 304 cracked plates obtained from the mentioned curves are given in Table 1.

**Table 1.** Mechanical properties of steel.

| Young's modulus E (GPa) | Yield stress $\sigma_y$ (MPa) | Poisson's ratio ν |
|---|---|---|
| 201 | 340 | 0.33 |

For executing post-buckling analysis in elastic-plastic case, the data of plastic region of the stress-strain curves were required. Therefore, as shown in Fig. 3(a-c), the stress-strain curves of three different thicknesses of stainless steel plates were determined for real and engineering cases.

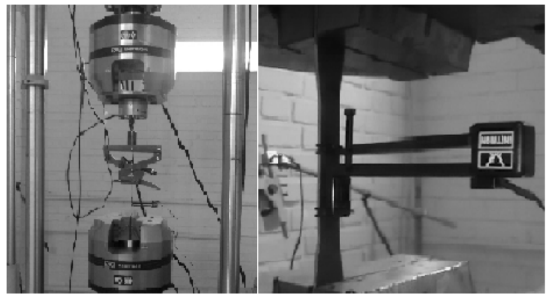

**Fig. 2.** Condition of mounting the standard tension specimens on INSTRON machine.

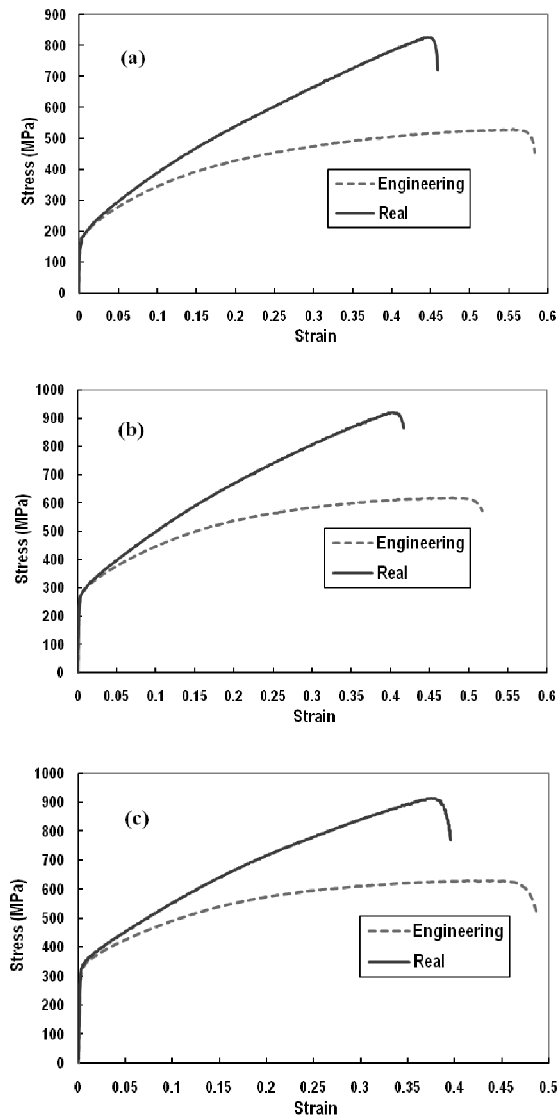


**Fig. 3.** Stress-strain curves for the plate thicknesses of: (a) 2 mm; (b) 3 mm; (c) 4 mm.

*2. 3. Measuring the initial imperfection*

Considering initial imperfection as an effective parameter in the buckling load, value of initial imperfection for all the specimens had to be experimentally measured before buckling test. This parameter was measured using an INSTRON servohydraulic machine test under load control with acceptable accuracy, as shown in Fig. 4(a and b). Initial curvature of the plates was obtained by pressing the specimen along the thickness direction using the actuator of machine test. Value of initial imperfection could be calculated by plotting the load-displacement curve. As an example, the load-displacement curve resulted from compressing the specimen CC-200-100-0.3-2-0 is shown in Fig. 5. It is obviously observed that the value of initial imperfection for this specimen was 0.325 mm, because the magnitude of force was increased with a steep slope without any increment in the displacement.

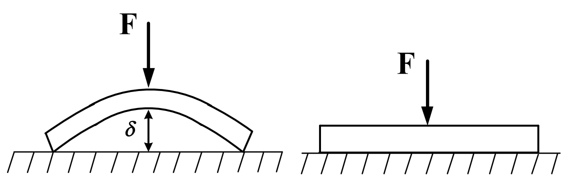


**Fig. 4.** Measuring the initial curvature of plates: (a) Before pressing the plate by force F (δ is initial imperfection); ( b) After pressing the plate by force F.

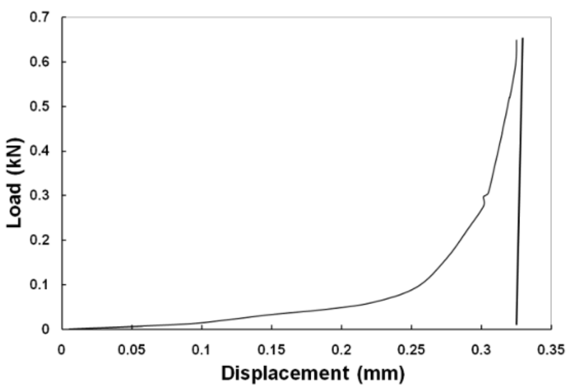


**Fig. 5.** Determining initial imperfection due to the curve obtained from experimental test.

*2. 4. Experimental test conditions*

The cracked plates were prepared for buckling analysis and the initial imperfection of the plates was regarded as the percentage of the plate thickness. Axial compression load was applied using INSTRON machine and the axial load and displacement of plates were extracted for plotting load-displacement curves to determine the critical load of buckling. Studies and investigations were carried out for the plates with two opposite clamped edges (boundaries 1 and 2 in Fig. 1(a)) and two opposite free edges (boundaries 3 and 4 in Fig. 1(a)) boundary conditions. The geometrical specimens that were experimentally studied are listed in Table 2. Load band of these specimens was equal to 0.5. In the specimen name column of Table 2, CC, UEC, and BEC stand for central crack, unilateral, and bilateral edge crack, respectively. Five next numbers in the specimen name column are the length and width of plate, crack length, plate thickness, and crack angle, respectively.

Furthermore, for investigating the effect of different load bands on critical buckling load, the axial load was applied with the following proportion of the plate width:

$$\varphi=\frac{2W_p}{2W}=0.25,\ 0.5,\ 0.75,\ 1 \qquad (1)$$

where φ stands for load band and $W_p$ is the width of applying load (Fig. 1). Figure 6 shows condition of applying axial compression load.

**Fig. 6.** Condition of applying axial compression load to the specimens using INSTRON machine.

**Table 2.** List of the geometrical specimens in experimental study.

| Specimen name | Crack length (mm) | Plate thickness (mm) | Crack angle (°) | Initial imperfection (mm) |
|---|---|---|---|---|
| CC-200-100-0-4-0 | 0 | 4 | 0 | 0.295 |
| CC-200-100-0.2-4-0 | 20 | 4 | 0 | 0.4554 |
| CC-200-100-0.3-4-0 | 30 | 4 | 0 | 0.29 |
| CC-200-100-0.3-4-30 | 30 | 4 | 30 | 0.2692 |
| CC-200-100-0.3-4-45 | 30 | 4 | 45 | 0.2857 |
| CC-200-100-0.3-4-60 | 30 | 4 | 60 | 0.235 |
| CC-200-100-0.3-4-90 | 30 | 4 | 90 | 0.29 |
| CC-200-100-0.5-4-90 | 50 | 4 | 90 | 0.5 |
| CC-200-100-0.7-4-90 | 70 | 4 | 90 | 0.2215 |
| CC-200-100-0.3-3-0 | 30 | 3 | 0 | 0.125 |
| CC-200-100-0.3-2-0 | 30 | 2 | 0 | 0.325 |
| UEC-200-100-0.2-4-0 | 20 | 4 | 0 | 0.4 |
| BEC-200-100-0.2-4-0 | 20 | 4 | 0 | 0.2654 |

## 3. Numerical study

Analytical solutions for determining the buckling and post-buckling behaviors of the cracked structures are very difficult. Consequently, most of the researchers have resorted to numerical methods for finding the answers to these problems. In this section, modeling of the buckling and post-buckling of plates under axial compression load along with central crack is studied using the numerical finite element method. Quantities of the critical buckling load of cracked plates were determined and also the graphs related to the behavior of post-buckling of these concerned plates were obtained using the mentioned method. Furthermore, effect of the mentioned parameters on the buckling phenomenon was investigated. Numerical modeling was done using the finite element software, called ABAQUS. To reach the concerned results, a series of linear and nonlinear numerical computations was done by using this software. Details of the general method for determining the buckling critical load and stages of estimating post-buckling behavior of the cracked plates by ABAQUS software were mentioned in [11].

Generally, post-buckling phenomenon is defined along with imperfection. It is worth mentioning that, at this stage, the quantity of the preliminary imperfection and also the data of plastic region related to the studied issue had to be defined for the software. As mentioned in the experimental study, the mechanical properties of stainless steel plates were determined for three thicknesses and the data of plastic region of the plates were extracted for the numerical study. Furthermore, the average imperfection of the experimental specimens which was about 0.3 mm was defined for the software as the imperfection of the plates in the numerical study. Geometrical specimens that were numerically studied are listed in Table 3.

### *3. 1. Mesh type*

In ABAQUS software, the appropriate type of element was the meshing of plates for the analysis of element buckling (S8R5) which was an 8-node element with 5 degrees of freedom in each node. One of the important stages in the analysis of cracked structures was their related meshing procedure, especially around the cracks. Appropriate mesh-setting for the analysis of cracked plates is shown in Fig. 7(a-d). Around 1200 elements were taken into consideration for each plate in all the analyses in order to result an acceptable convergence.

### *3. 2. Buckling mode shapes of the cracked plates*

As pointed out earlier, the concerned mode shape at the preliminary buckling stage could be resulted. The first and second mode shapes related to central cracked plates under compression load for 0° of crack angle and fixed-ends boundary conditions is shown in Fig. 8(a and b).

Figure 9 demonstrates the variation of Von Mises stress and deformation of the plate at three points of the load-displacement curve caused by the post-buckling of central cracked plate for $0^o$ crack angle and relative crack length of 0.2 under axial compression load. It is observed in Fig. 9 that the deformation complies with the changes of the first mode shape, meaning that it is an acceptable deformation, because deformation always follows the mode shape which has the least eigenvalue (critical load) and this value adopts the least quantity for the first mode shape.

**Table 3.** List of the geometrical specimens in numerical study.

| Specimen name | Crack length (mm) | Plate thickness (mm) | Crack angle (°) |
|---|---|---|---|
| CC-200-100-0-4-0 | 0 | 4 | 0 |
| CC-200-100-0.1-4-0 | 10 | 4 | 0 |
| CC-200-100-0.3-4-0 | 30 | 4 | 0 |
| CC-200-100-0.5-4-0 | 50 | 4 | 0 |
| CC-200-100-0.1-4-30 | 10 | 4 | 30 |
| CC-200-100-0.2-4-30 | 10 | 4 | 0 |
| CC-200-100-0.3-4-30 | 30 | 4 | 30 |
| CC-200-100-0.5-4-30 | 50 | 4 | 30 |
| CC-200-100-0.1-4-45 | 10 | 4 | 45 |
| CC-200-100-0.3-4-45 | 30 | 4 | 45 |
| CC-200-100-0.5-4-45 | 50 | 4 | 45 |
| CC-200-100-0.1-4-60 | 10 | 4 | 60 |
| CC-200-100-0.3-4-60 | 30 | 4 | 60 |
| CC-200-100-0.5-4-60 | 50 | 4 | 60 |
| CC-200-100-0.1-4-90 | 10 | 4 | 90 |
| CC-200-100-0.3-4-90 | 30 | 4 | 90 |
| CC-200-100-0.5-4-90 | 50 | 4 | 90 |
| CC-200-100-0.3-3-0 | 30 | 3 | 0 |
| CC-200-100-0.3-2-0 | 30 | 2 | 0 |
| UEC-200-100-0.2-4-0 | 20 | 4 | 0 |
| BEC-200-100-0.2-4-0 | 20 | 4 | 0 |

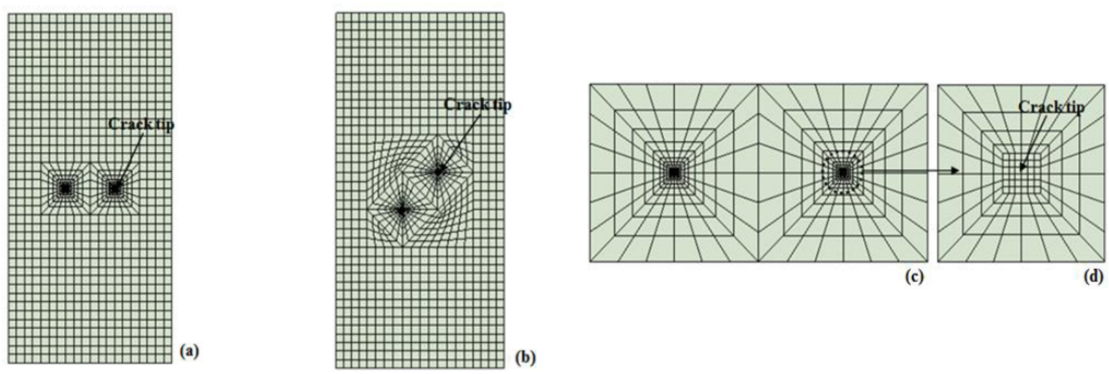


**Fig. 7.** Mesh-setting of the cracked plate for buckling analyses: (a) $0^o$; (b) $45^o$; (c); and (d) crack tip mesh detail.


**Fig. 8.** Mode shapes of CC-200-100-0.2-4-0 specimen (a) first mode shape, and (b) second mode shape.

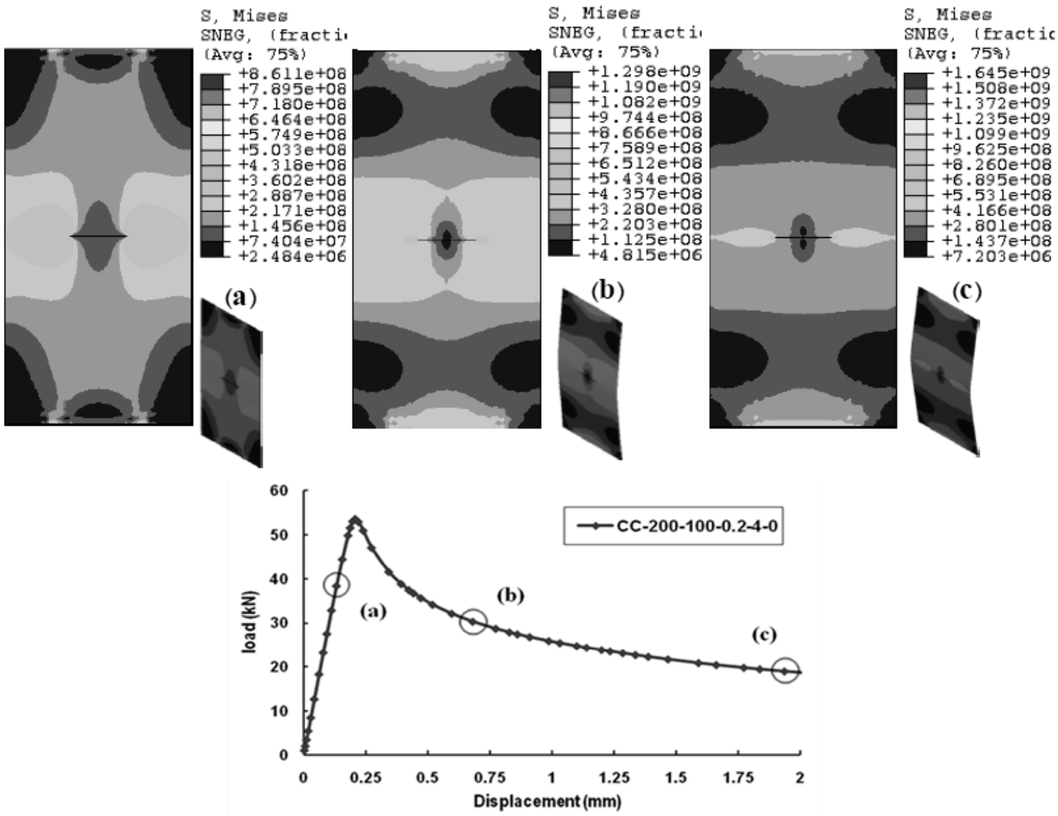


**Fig. 9.** Variation of stress and deformation at three points of the load-displacement curve for CC-200-100-0.2-4-0 specimen.

## 4. Results and discussion

### *4. 1. Experimental results*

The experimental analyses were carried out for considering the effect of the following parameters on the buckling phenomenon:

#### *4. 1. 1. Effect of relative crack length*

In Fig. 10(a), effects of the crack length increment on buckling load for $0^o$ crack angle can be observed. The curves indicate that increase of the crack length caused decrease in the quantity of the buckling critical load for $0^o$ crack angle. It is also observed that there was no considerable difference between the critical buckling load of the plate with relative crack lengths of 0.2 and 0.3 .The reason can be the initial imperfection of relative crack length of 0.2 which was about twofold of relative crack length of 0.3 and decreased the buckling critical load of plate with the crack length of 20 mm.

Fig. 10(b) demonstrates the effect of crack length on buckling load for 90° crack angle. Although there must be no significant difference between the critical buckling load of different crack lengths for 90° crack angle, initial imperfection in the plate with the crack length of 50 mm yielded considerable decrease in the critical buckling load of the specimen. It is also evident that a little time after buckling of as much as 1.25 mm, the curves were made convergent to a definite extent for the whole graphs. It is also seen that the increase of crack angle reduced the effect of the crack existence in such a way that, for the crack with 0° angle, the increase of the dimensionless crack length caused considerable decrease in the critical load of buckling, while this decrease in 90° angle was not so significant.

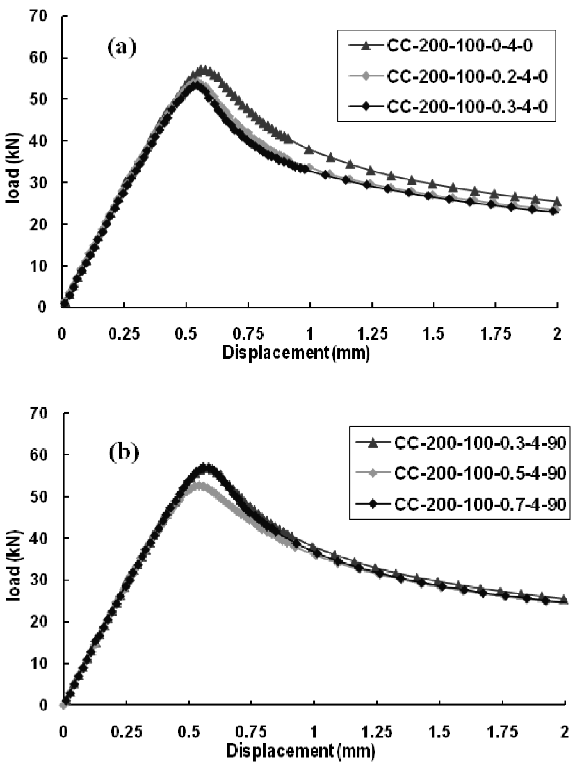


**Fig. 10.** Effect of crack length on the load-displacement curve for buckling and post-buckling of the cracked plates with the crack angle of: (a) 0°, and (b) 90° in the experimental study.

*4. 1. 2. Effect of crack angle*

Load-displacement curves for different crack angles are shown In Fig. 11. It is observed that the increase of the crack angle caused increase of buckling critical load. There was inconsistency in the plate with 90° crack angle, because the initial imperfection of this plate was about 0.29 mm which was more than the imperfection of the plate with 60° crack angle and caused decrease in the buckling critical load. This point indicates that imperfection mostly influences the critical buckling load, while the increase of the crack angle causes decrease in the effect of crack presence.

*4. 1. 3. Effect of crack position*

In Fig. 12, effect of the crack position on the load-displacement curve for the buckling critical load is studied. It is observed that the central cracked plate had minimum critical load of buckling. The unilateral edge crack must have maximum buckling critical load; however, because the initial imperfection of unilateral edge crack was greater than bilateral one, the critical buckling load of unilateral edge crack decreased.

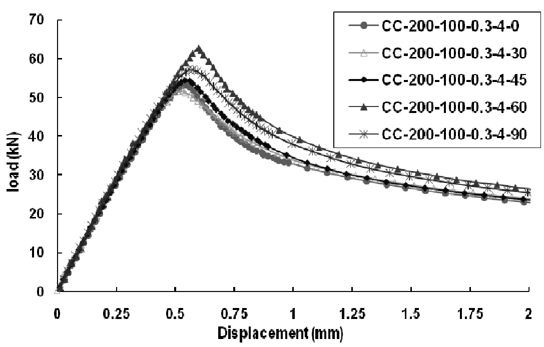


**Fig. 11.** Effect of crack angle on the load-displacement curve for buckling and post-buckling of the cracked plates in the experimental study.

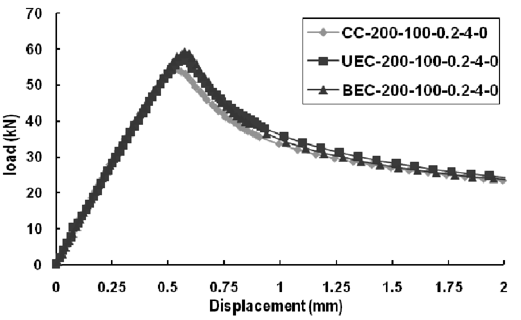


**Fig. 12.** Effect of crack position on the load-displacement curve for buckling and post-buckling of the cracked plates in the experimental study.

*4. 1. 4. Effect of plate thickness*

In Fig. 13, the load-displacement curve for three plate thicknesses is presented. It is evident that the buckling critical load increased considerably by the increase of the thickness in such a way that the critical load of buckling amounted to 6.9 kN in 2 mm plate thickness and to 53 kN in 4 mm thickness of plate.

*4.1.5. Effect of load band*

For investigating the effect of the load band on the buckling of cracked plate, the load-displacement curves are shown for different proportions of load band in Fig. 14. It is evident that increasing the load band proportion from 0.25 to 1 caused the buckling phenomenon to happen later.

*4. 2. Numerical results*

Considerable points from the load displacement-curves resulted could be obtained from the finite element numerical method. To continue the numerical results, effect of the parameters on the quantities of the critical buckling load is investigated.

In Figs. 15-19, effect of the relative crack length, crack angle, crack position, plate thickness, and load band on the load displacement is studied, respectively. In Fig. 15, the load-displacement curves are shown for the crack-less plate and for plates with various crack lengths. The curves indicate that the increase in the crack length resulted in considerable decrease in the quantity of critical buckling load and the trend of curves was in an almost parallel way. Fig. 16 shows the load-displacement curves for different crack angles. It is observed that the increase of the crack angle yielded an increment in buckling critical load. It is obviously seen in Fig. 17 that there was no considerable difference between the load-displacement curves of central and edge cracks in the numerical study and the changes in the position of the crack from central crack to the edge one increased the critical load of buckling. It is observed in Fig. 18 that an increase in the plate thickness caused significant increase in the quantity of critical buckling load. Also, the load-displacement curves in Fig. 19 which were plotted for different load band proportions demonstrate that decreasing the load band from 1 to 0.25 caused considerable decrease in the critical load of buckling.

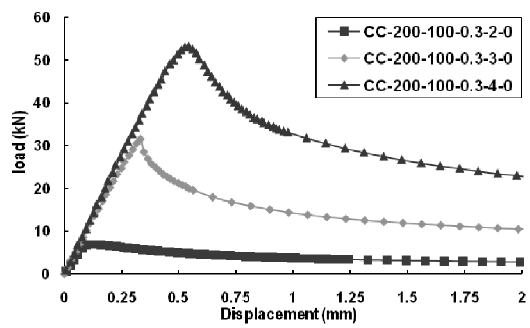


**Fig. 13.** Effect of plate thickness on the load-displacement curve for buckling and post-buckling of the cracked plates in the experimental study.

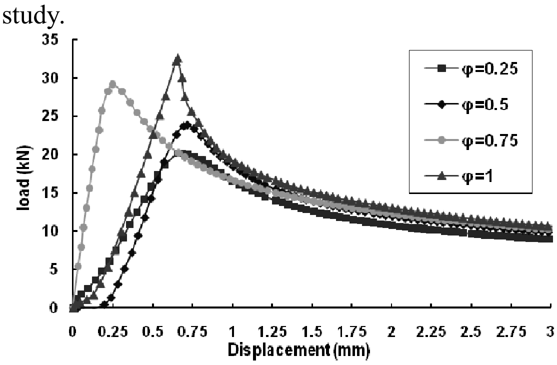


**Fig. 14.** Effect of load band on the load-displacement curve for buckling and post-buckling of the cracked plates in the experimental study.

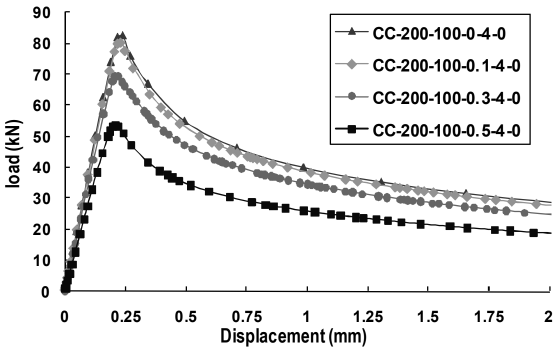


**Fig. 15.** Effect of crack length on the load-displacement curve for buckling and post-buckling of the cracked plates (φ=0.5) in the numerical study.

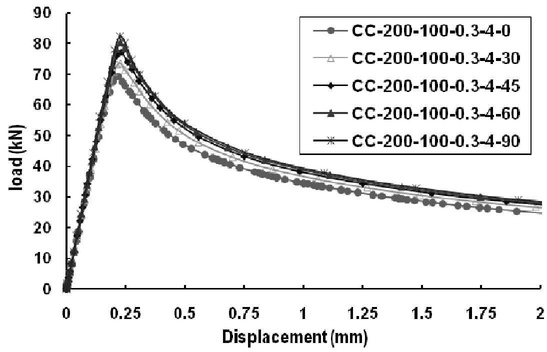


**Fig. 16.** Effect of crack angle on the load-displacement curve for buckling and post-buckling of the cracked plates (φ=0.5) in the numerical study.

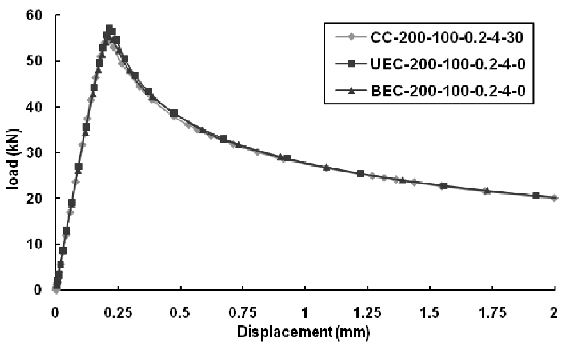


**Fig. 17.** Effect of crack position on the load-displacement curve for buckling and post-buckling of the cracked plates (φ=0.5) in the numerical study.

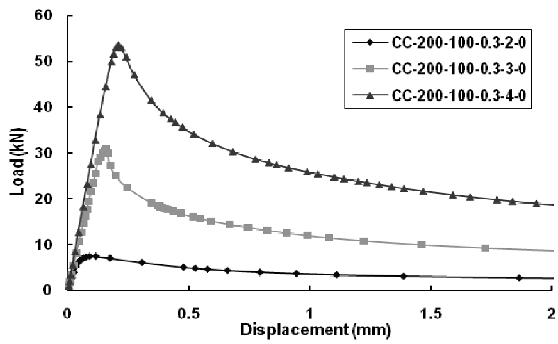


**Fig. 18.** Effect of the plate thickness on the load-displacement curve for buckling and post-buckling of the cracked plates (φ=0.5) in the numerical study.

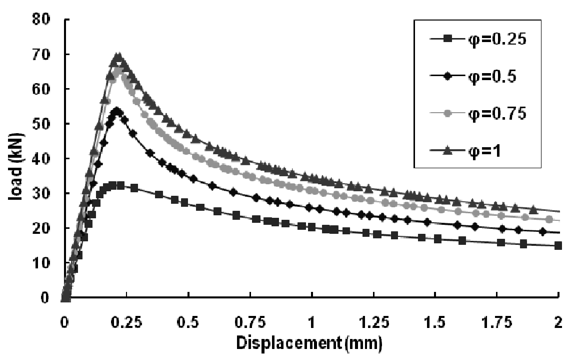


**Fig. 19.** Effect of load band on the load-displacement curve for buckling and post-buckling of the cracked plates in the numerical study.

*4. 3. Comparison of results*

The numerical predictions and experimental results of critical buckling load for different specimens and the percent of the difference between these two methods are listed in Table 4. It is observed that the maximum difference between the numerical and experimental critical buckling loads was less than 9.4% and the minimum difference was 0.14%. Because of the existence of different quantities of imperfection between numerical and experimental specimens, the average of 4.04% for the difference between the critical buckling loads of these two methods was acceptable.

**Table 4.** Comparison of the numerical and experimental critical load of buckling and the percent of difference between the results of two methods.

| Specimen name | Buckling load (kN) | | percent of difference |
|---|---|---|---|
| | Exp. | Num. | |
| CC-200-100-0-4-0 | 57.425 | 56.2 | 2.1 |
| CC-200-100-0.2-4-0 | 54.247 | 51.04 | 5.9 |
| CC-200-100-0.3-4-0 | 53.267 | 53.628 | 0.69 |
| CC-200-100-0.3-4-30 | 51.764 | 54.82 | 5.9 |
| CC-200-100-0.3-4-45 | 54.43 | 55.94 | 2.7 |
| CC-200-100-0.3-4-60 | 62.777 | 57.91 | 7.75 |
| CC-200-100-0.3-4-90 | 57.208 | 58.19 | 1.7 |
| CC-200-100-0.5-4-90 | 52.647 | 51 | 3.1 |
| CC-200-100-0.7-4-90 | 56.929 | 51.58 | 9.4 |
| CC-200-100-0.3-3-0 | 31.565 | 30.5 | 3.6 |
| CC-200-100-0.2-3-0 | 23.88 | 25.12 | 4.9 |
| CC-200-100-0.3-2-0 | 6.9688 | 7.4 | 6.1 |
| UEC-200-100-0.2-4-0 | 57.142 | 57.06 | 0.14 |
| BEC-200-100-0.2-4-0 | 59.278 | 56.82 | 4.1 |

## 5. Conclusions

The numerical predictions and experimental results indicated that:

1. Generally, the existence of crack in plates caused decrease in the value of buckling critical load, while having no considerable effect on the post-buckling behavior of plate and the increase of crack length caused considerable decrease in the general buckling load.
2. Increase of crack angle from $0^o$ to $90^o$ resulted in the considerable increase of the buckling critical load; meaning that increasing the crack angle decreased the effect of the crack presence and this effect can be ignored in the angles near to $90^o$.
3. Changes of crack position from central to edge cracks increased the critical load of buckling. Central cracked plate had the minimum critical load of buckling and the unilateral edge crack had the maximum one. It is mentioned that these variations were not considerable.
4. Changes in the plate thickness significantly affected the buckling critical load, meaning that increasing the plate thickness caused considerable increase in the quantity of buckling load.
5. In this paper, effect of load band on the buckling phenomenon was investigated and it was observed that decreasing the proportion of load band from 1 to 0.25 caused a significant decrease in the critical load of buckling.
6. Average of 4.04% for the difference between the critical buckling load of numerical and experimental results was acceptable.
7. In cracked plates under axial compression load, the increase of the initial imperfection caused decrease in the critical load of buckling. This parameter had the greatest effect compared with other parameters on the buckling load in the experimental study.

**References**

[1] G. C. Sih and YD. Lee, “Tensile and compressive buckling of plates weakened by cracks”, *Theoritical and Applied Fracture Mechanics*, Vol. 6, No. 2, pp. 129-138, (1986).

[2] D. Shaw and Y. H. Huang, “Buckling behavior of a central cracked thin plate under tension”, *Engineering Fracture Mechanics,* Vol. 35, No. 6, pp. 1019-1027, (1990).

[3] E. Riks, C. C. Rankin and F. A. Bargon, “Buckling behaviour of a central crack in a plate under tension”, *Engineering Fracture Mechanics,* Vol. 43, No. 4, pp. 529-548, (1992).

[4] A. N. Guz and M. S. h. Dyshel, “Fracture and buckling of thin panels with edge crack in tension”, *Theoritical and Applied Fracture Mechanics,* Vol. 36, No. 1, pp. 57-60, (2001).

[5] Y. V. Satish Kumar and J. K. Paik, “Buckling analysis of cracked plates using hierarchical trigonometric functions”, *Thin-Walled Structure,* Vol. 42, No. 5, pp. 687-700, (2004).

[6] R. Brighenti, “Numerical buckling analysis of compressed or tensioned cracked thin plates”, *Engineering. Structure,* Vol. 27, No. 2, pp. 265-276, (2005).

[7] R. Brighenti, “Buckling of cracked thin-plates under tension or compression”, *Thin-Walled Structure,* Vol. 43, No. 2, pp. 209-224, (2005).

[8] R. Brighenti, “Buckling sensitivity analysis of cracked thin plates under membrane tension or compression loading”, *Nuclear Engineering and Design,* Vol. 239, No. 6, pp. 965-980, (2009).

[9] M. M. Alinia, S. A. A. Hoseinzadeh and H. R. Habashi, “Influence of cracks on buckling and post- buckling behavior of shear panels”, *Thin-Walled Structure,* Vol. 45, No. 4, pp. 422-431, (2007).

[10] M. M. Alinia, S. A. A. Hoseinzadeh and H. R. Habashi, “Numerical modeling for buckling analysis of cracked shear panels”, *Thin-Walled Structure,* Vol. 45, No. 12, pp. 1058-1067, (2007).

[11] M. Shariati and A. M. Majd Sabeti, “Numerical Buckling and post-buckling of cracked plates under axial compression load”, *Journal of Aerospace Engineering*, Vol. 2, No. 2, pp. 84-90, (2009).